

High-resolution Autoreactive Epitope Mapping and Structural Modeling of the 65 kDa Form of Human Glutamic Acid Decarboxylase

Heather L. Schwartz^{1,2}, John-Marc Chandonia³, Shera F. Kash¹
 Jamil Kanaani¹, Evelyn Tunnell¹, Antoinette Domingo¹, Fred E. Cohen³
 J. Paul Banga⁴, Anne-Marie Madec⁵, Wiltrud Richter⁶
 and Steinunn Baekkeskov^{1,2*}

¹Departments of Microbiology/
 Immunology and Medicine
 Hormone Research Institute
 University of California
 San Francisco, CA, 94143-
 0534, USA

²Graduate Program in
 Immunology, University of
 California, San Francisco, USA

³Department of Cellular and
 Molecular Pharmacology
 University of California
 San Francisco, CA, 94143-
 0450, USA

⁴Department of Medicine
 King's College School of
 Medicine, London, SE5 9PJ
 United Kingdom

⁵INSERM Unit 449, R.
 Laennec Faculty of Medicine
 University of Lyon, 69372 Lyon
 Cedex 08, France

⁶Department of Internal
 Medicine, University of Ulm
 D-89070, Ulm, Germany

*Corresponding author

The smaller isoform of the GABA-synthesizing enzyme, glutamic acid decarboxylase 65 (GAD65), is unusually susceptible to becoming a target of autoimmunity affecting its major sites of expression, GABA-ergic neurons and pancreatic β -cells. In contrast, a highly homologous isoform, GAD67, is not an autoantigen. We used homolog-scanning mutagenesis to identify GAD65-specific amino acid residues which form autoreactive B-cell epitopes in this molecule. Detailed mapping of 13 conformational epitopes, recognized by human monoclonal antibodies derived from patients, together with two and three-dimensional structure prediction led to a model of the GAD65 dimer. GAD65 has structural similarities to ornithine decarboxylase in the pyridoxal-5'-phosphate-binding middle domain (residues 201-460) and to dialkylglycine decarboxylase in the C-terminal domain (residues 461-585). Six distinct conformational and one linear epitopes cluster on the hydrophilic face of three amphipathic α -helices in exons 14-16 in the C-terminal domain. Two of those epitopes also require amino acids in exon 4 in the N-terminal domain. Two distinct epitopes reside entirely in the N-terminal domain. In the middle domain, four distinct conformational epitopes cluster on a charged patch formed by amino acids from three α -helices away from the active site, and a fifth epitope resides at the back of the pyridoxal 5'-phosphate binding site and involves amino acid residues in exons 6 and 11-12. The epitopes localize to multiple hydrophilic patches, several of which also harbor DR*0401-restricted T-cell epitopes, and cover most of the surface of the protein. The results reveal a remarkable spectrum of human auto-reactivity to GAD65, targeting almost the entire surface, and suggest that native folded GAD65 is the immunogen for autoreactive B-cells.

© 1999 Academic Press

Keywords: type 1 diabetes; autoantigen; B-cell epitopes; two-dimensional structure; three-dimensional structure

Introduction

Two non-allelic isomers of the enzyme glutamate decarboxylase, GAD65 and GAD67, synthesize the major inhibitory neurotransmitter GABA (γ -amino butyric acid in mammals (Bu *et al.*, 1992; Erlander *et al.*, 1991). The two enzymes appear to have evolved from a common precursor, share an identical exon-intron structure (Bu & Tobin, 1994) and are 76% identical and 87% similar throughout the last 12 exons (exons 5-16, residues 174-585). Within

Abbreviations used: GAD, glutamic acid decarboxylase; GABA, γ -amino butyric acid; PLP, pyridoxal 5'-phosphate; 1ORD, ornithine decarboxylase; 2DKB, dialkylglycine decarboxylase; BSA, bovine serum albumin; Mab, monoclonal antibody.

E-mail address of the corresponding author:
 s_baekkeskov@biochem.ucsf.edu

the N-terminal region, however, the two isomers differ significantly, with 22% identity in exons 1-3 and 49% identity in exon 4. The larger isomer, GAD67, is a soluble hydrophilic enzyme present mainly in the cell body of neurons (Kaufman *et al.*, 1991) and in the cytosol of rat pancreatic β -cells (Christgau *et al.*, 1991). The GAD65 isoform is synthesized as a hydrophilic soluble molecule, which undergoes several hydrophobic modifications and is reversibly anchored to the membrane of synaptic vesicles in neurons and synaptic-like microvesicles in β -cells (Christgau *et al.*, 1992; Reetz *et al.*, 1991). The strategic and dynamic location of this isoform to the membrane of vesicles that accumulate and secrete its product, GABA, is consistent with its role in providing GABA for rapid secretion to fine tune inhibitory neurotransmission (Kash *et al.*, 1997, 1999; Hensch *et al.*, 1998).

GAD65, unlike GAD67, has unique features which make it unusually susceptible to becoming an autoantigen. In human type 1 (insulin-dependent) diabetes, which develops because of a T-cell-mediated destruction of pancreatic β -cells, GAD65 antibodies are an early marker of autoimmune destruction in 70-80% of patients (Baekkeskov *et al.*, 1990). GAD65 autoantibodies can be detected up to several years before the clinical onset of disease (Baekkeskov *et al.*, 1987), which may occur when $\geq 80\%$ of β -cells are destroyed (Martin & Lacey, 1963). Although antibodies to GAD67 are detected in 11-18% of patients (Hagopian *et al.*, 1993), they seem to represent antibodies to shared epitopes with GAD65. Antibodies to GAD65 can persist for many years following the clinical onset of diabetes (Christie *et al.*, 1990), even when no β -cell activity in the form of blood C-peptide can be measured. Thus, GAD65 autoreactivity may persist as part of a chronic inflammation that may destroy new β -cells as they form from the pancreatic duct and/or are received as a pancreas or islet transplant.

In the non-obese diabetic (NOD) mouse model of diabetes, GAD65 is the first known target of autoimmune Th1 CD4+ T-cell responses (Kaufman *et al.*, 1993; Tisch *et al.*, 1993), and GAD65-specific Th1 CD4+ T-cell clones can induce disease when transferred into NOD-SCID mice (Zekzer *et al.*, 1998). GAD65 is also an autoantigen in $>95\%$ of patients suffering from a rare autoimmune neurological disorder, stiff-man syndrome (SMS), that affects GABA-ergic neurons (Kim *et al.*, 1994; Solimena *et al.*, 1990). SMS is characterized by a high coincidence with type 1 diabetes (30-40%), and with autoimmune thyroid disorders (Lorish *et al.*, 1989).

To assess the structural requirements and diversity of GAD65-specific autoimmune epitopes we have mapped in detail the GAD65-specific residues of one linear and 13 conformational epitopes recognized by 16 human monoclonal antibodies derived from human patients. For this purpose we have used homolog-scanning mutagenesis (Cunningham *et al.*, 1989) together with two and three-dimen-

sional structure modeling. Three-dimensional modeling of GAD65 predicts that all the epitopes are within charged hydrophilic patches on the surface of the native molecule, and together cover almost every possible surface region of GAD65.

Results

Biochemical analysis of autoreactive epitopes in GAD65

The 16 human monoclonal antibodies used in this study are specific for GAD65 and do not recognize GAD67 (Madec *et al.*, 1996; Richter *et al.*, 1993). Yet the epitopes for 12 of these antibodies have been localized to the middle and C-terminal regions of GAD65 (Richter *et al.*, 1993; Syren *et al.*, 1996; Tremble *et al.*, 1997) which are 76% identical with GAD67 (Bu *et al.*, 1992). Because of the identical exon-intron structure (Bu & Tobin, 1994), and the high degree of homology between GAD65 and GAD67, we reasoned that swapping of exons or smaller regions in the areas of high homology was likely to have a local rather than a widespread conformational effect on each protein. Consistent with this hypothesis, the large swap mutants used in this study (1-242, 242-439, 451-585) have been shown to be enzymatically active when expressed in COS-7, demonstrating that they fold correctly (J.K., H.L.S., & S.B., unpublished results). Here, GAD67 was used as a negative reference molecule in homolog-scanning mutagenesis to identify GAD65-specific sequences/amino acids involved in epitope recognition.

Generation of chimeric GAD65/67 constructs and protein expression

A panel of 23 GAD65/67 chimeras was generated, including multiple or individual exon swaps covering the N-terminal, middle, or C-terminal region of GAD65 (Figure 1). Of these, 19 mutants could be expressed at sufficient levels for analysis. For detailed mapping of epitopes, 35 point mutants were generated, substituting GAD65-specific amino acids with the corresponding GAD67 residues or, in one case, with alanine because the substitution mutant was not expressed. Two mutants were generated that exchanged conserved pyridoxal 5'-phosphate (PLP) binding site residues for alanine, and three mutants were generated that introduced a GAD65-specific residue into GAD67 (Figure 1). Most of the GAD65 point mutations involved hydrophilic residues to avoid destabilizing the core of the protein.

A complete or partial loss of antibody reactivity by a point mutation suggests that GAD65-specific sequences required for contact with the antibody or for maintaining a correct epitope conformation have been removed.

		Exon 1	*	Exon 2	*
GAD65	1	MA--TPGSSGFWSFGSENGSGDSENPGTARAWCQVAQKFTGGIGNKLICAL			
GAD67	1	SS S -ATS NAGA PNTNLR T YDN G HGC RKL L I GF			
		38	Exon 3		
GAD65	48	LYGDAEKPAES---GGSQPPRAAARKAACACDQKPCSCSKVDVNYAFLHA			
GAD67	51	QRTNSLEEK RLVSFAKERQSSKNLLS ENSDRDARFRRTETETDFSN F			
		100	Exon 4	134	
GAD65	95	TDLLPACDGERPTLALLQDVMNILLQYVVKSFDRSTKVIDFHYPNELLQ-			
GAD67	101	R KN EQ VQ LE VD N R T L H HQ EG			
		195	Exon 5		
GAD65	143	--EYTWELADQPQNLEEILMHCQTTLKYAIKTGHPRYFNQLSTGLDMVGL			
GAD67	151	MEGF L S H E S Q VD RD GVR F II			
		242	Exon 6	282	
GAD65	192	AADWLTSTANTNMFTYEIAPVFLLE ^Y VTLKKMREIIGW ^F GGSGDGIFSP			
GAD67	201	GE M Q I V SSKD			
		308	Exon 7	365	
GAD65	242	GGAISNMYAMM ^T ARFK ^M FPEVK ^E EKGMAALPRLIAFTSE ^H SHFSLKKGAAA			
GAD67	251	SI A Y Y T V K VL O Y I AG			
		413	Exon 8	439	
GAD65	292	LCIGTDSVILIKCDER ^G KMIP ^S DL ^E RRILEAKQKGYVPFL ^V SATAGTTVY			
GAD67	301	F N N I A F AK Y N			
		451	Exon 9	483	
GAD65	342	GAFDPL ^L AVADICK ^K KY ^K IWMHVD ^A AWGGLLMSRKHKWKLSGVERANSVT			
GAD67	351	IQEI E NL L RH N I			
		512	Exon 10	532	
GAD65	392	WNP ^H KMMGVPLQCSALLVREE ^G LMQNCNQMHASYL ^F QQDKHYDLSYD ^T TGD			
GAD67	401	L I K K IL G C G P Q V			
		550	Exon 11	556	
GAD65	442	KALQCGRHV ^D VFK ^L WLMWRAKGT ^T GFGAH ^V DKCLELAEYLY ^N IKNREGY			
GAD67	451	I I F K V NQIN AK EF			
		550	Exon 12	556	
GAD65	492	EMVFD ^G K ^P QHTNVCFWYI ^P SLR ^T LED ^N FERMSRL ^G KVAP ^V IKAR ^M MEY ^G			
GAD67	501	N E E Q GVPSPQREX H K L S			
		550	Exon 13	556	
GAD65	542	TTMV ^S YQP ^L GDKVNF ^F FRMVISNPAAT ^H QDIDFLIEEIERLGQDL			
GAD67	551	G Q A Q S			

Figure 1. GAD65 and GAD67 sequences and generation of mutants. Shaded boxes correspond to GAD65/67 point mutants. Vertical bars indicate boundaries for 65/67 swap mutants. Intron locations are marked by asterisks (*). Highly conserved amino acid differences (including GAD65 G and A substitutions) are shown in grey. Chimeric proteins are described by the range of amino acids in GAD65 which were swapped with the corresponding region of GAD67. GAD65/67 chimeric proteins: 1-102, 1-134^a, 1-242^b, 134-242, 242-282^b, 242-308^b, 242-439^b, 282-308, 308-365, 366-413^a, 366-439^b, 413-439, 446-525^a, 451-512^a, 451-585, 483-499, 512-585, 515-530^a, 532-540, 532-550, 540-550, and 556-585^b. GAD65/67 point mutants: Y218Q, E264T, H280Q^b, P231S/S234D, I253A/M258Y, L315F, S314A/R317A, S314A, R317A, L331Y/S333N, L348Q, K355E/K358N^a, K355E, K358N, H470Q, T465V/D472, N483A, I484 K, D496N/Q500E, K498E, P511Q, T515G, E517P, N519S, E520P, E521Q, M523R^a, M523A, S524E, S527H, V532 K, R536L, Y540S, H568Q^b, and Q569S. GAD65-alanine mutants: H395A/K396A and M523A. GAD67 chimeric proteins: 67/242-366, 67/T273E, 67/A326R, 67/N367 K. (a) Expression levels as measured by cpm in GAD6 (a linear epitope) immunoprecipitates are too low for immunoprecipitation analysis; (b) mutants are conformationally unstable and can lose 10-30% of wild-type reactivity with GAD1 and/or other conformational Mabs that bind outside the mutated area during the course of an immunoprecipitation experiment (eight hours). In contrast, reactivity with GAD6 that recognizes a linear epitope is not affected demonstrating that the mutant is expressed at similar levels as wild-type protein.

Large domain swaps define five distinct epitope patterns amongst the human monoclonal antibodies spanning the entire GAD65 molecule

We first analyzed the reactivity of the human monoclonal antibodies (Mabs) to a panel of three GAD65/67 chimeric proteins in which either residues 1-242, 242-439 or 451-585 of GAD65 were replaced with the corresponding region in GAD67. These analyses revealed five major patterns of human MAb recognition (Figure 2): (1) DPB and DPD are dependent on the residues 1-242 region of GAD65 but are unaffected by either middle or C-terminal region swaps; (2) b96, M4, M6, and M10 are dependent on the middle region of GAD65 (residues 242-439), but are unaffected by either the 1-242 or C-terminal swaps; (3) b78, DPA, M1, M2, M3, M5, and M7 are dependent on the C-terminal region of GAD65 (residues 451-585) but are unaffected by the other swaps; (4) M8, M9 lose reactivity with both the 1-242 and 451-585 residue swaps, but are unaffected by the middle region swap; and (5) DPC loses reactivity with both the 1-242 and 242-439 residue swaps, but is unaffected by the C-terminal swap. Thus the 16 autoreactive human MABs define epitopes in all three regions of the GAD65 molecule, as well as epitopes that span two regions. A recent study that assessed the ability of the M1-M10 antibodies to block the binding of each other to frozen sections of human pancreas revealed three distinct blocking groups (P. Söhnlein *et al.*, unpublished results). M4, M6 and M10 block each other, but none of the other antibodies. Similarly, M1 and M3 block each other but none of the other antibodies. M2, M5, M7, M8, and M9 form a distinct blocking group amongst the antibodies dependent on the C-terminal region. Within this last blocking group, M8 but not M9 can block M2, suggesting that M8 and M9 recognize distinct epitopes in this region. Antibody footprinting analysis of the M1-M10 antibodies showed identical patterns for M1 and M3 and for M8 and M9. All the other antibodies displayed a unique pattern (results not shown), suggesting that they bind to distinct epitopes; this is further supported by detailed mapping of the epitopes.

Detailed mapping of autoreactive epitopes

The human Mabs were analyzed for reactivity with smaller swap mutants within the epitope regions and with amino acid substitution mutants introducing non-conserved GAD67 residues into GAD65 in the relevant areas of the molecule.

The data shown in Figure 3 revealed that M4, M6, M10, b96 and DPC define five distinct epitopes in the middle region (residues 242-439, exons 7-13). M6 and M10 are dependent on GAD65-specific amino acids in exon 7 (residues 242-282) and E264 is a critical amino acid for M10 but not M6 binding (Figure 3(a)). Similarly, M4 and b96 map to a single swap area covering exons 9 and 10

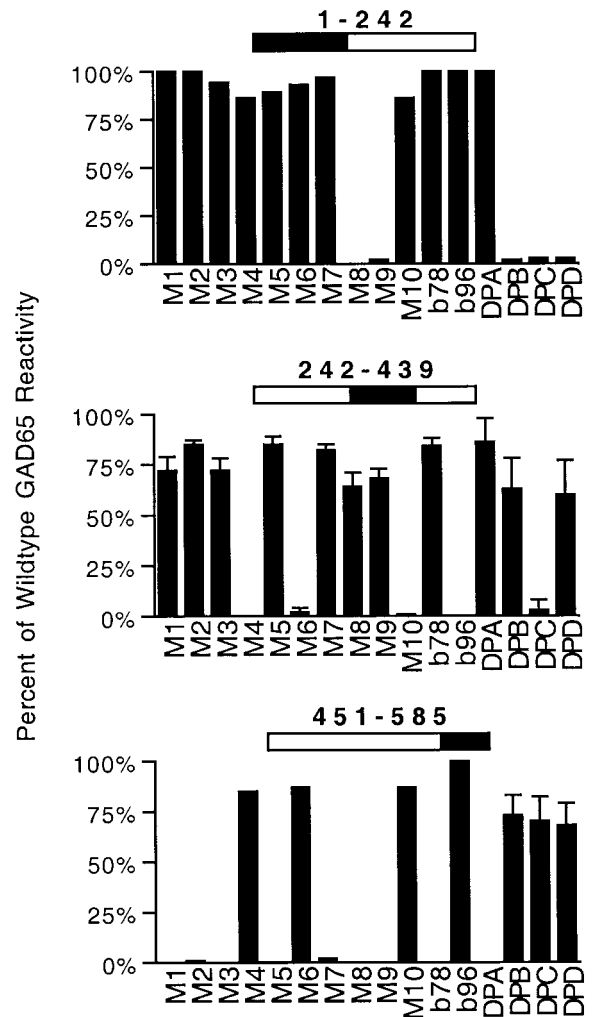


Figure 2. Immunoprecipitation analyses of GAD65 residues 1-242, 242-439, and 451-585 swap mutants reveal five distinct epitope patterns for autoreactive human MABs. The [³⁵S]methionine labeled GAD65/67 swap mutants were immunoprecipitated with each of the shown antibodies. The 65 and 67 regions are indicated in white and black, respectively, for each mutant. The results are expressed as a percentage of cpm immunoprecipitated in parallel using wild-type GAD65. The bars represent an average of three to six experiments. Error bars are shown except where standard error means are negligible (<2%). The epitopes of five human Mabs, DPB, DPC, DPD, M8, and M9 are lost by the residues 1-242 residue swap. Five human MABs, M4, M6, M10, b96, and DPC lose reactivity by the residues 242-439 swap. Nine human MABs, M1, M2, M3, M5, M7, M8, M9, b78, and DPA require residues 451-585 in GAD65. M8 and M9 are lost by both the 1-242 and C-terminal swaps, while DPC is lost by both the 1-242 and middle region swap.

(residues 308-365; Figure 3(b)) and K358 is a critical binding residue for M4 but not b96 binding (Figure 3(b)). For M6 and b96, no single point mutation within the critical regions resulted in a significant loss of reactivity, suggesting that for those antibodies GAD65-specific residues may be

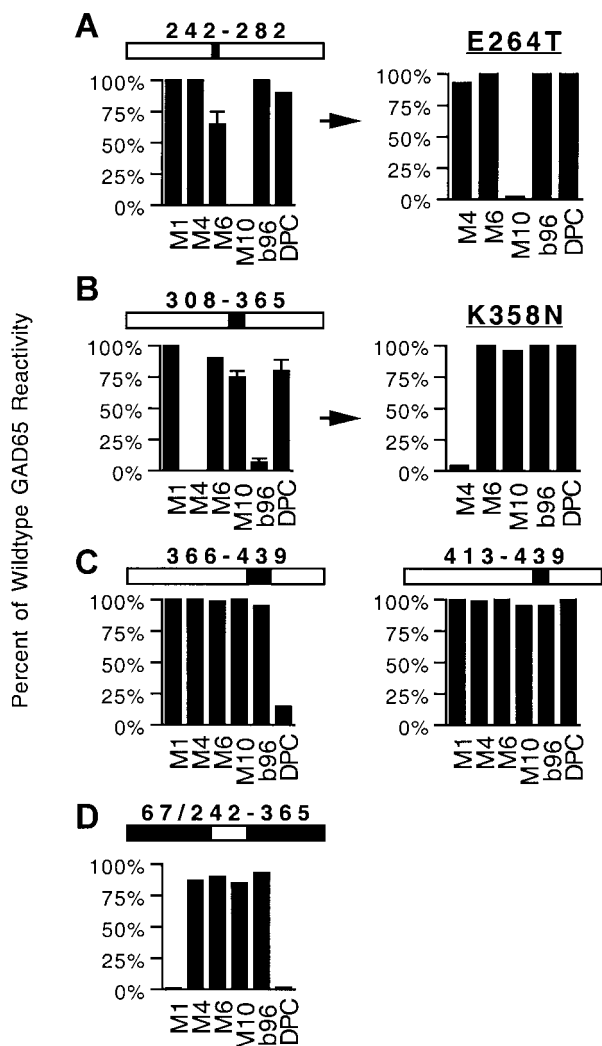


Figure 3. M6, M10, M4, b96 and DPC define five distinct epitopes in the middle region (residues 200-439) of GAD65. Immunoprecipitation of [35 S]methionine labeled swap and point mutants in the middle region. The 65 and 67 regions are indicated in white and black, respectively, for each swap mutant. The results are expressed as a percentage of cpm immunoprecipitated in parallel using wild-type GAD65. The bars represent an average of three to six experiments. Error bars are shown for mutations that had a significant effect on antibody binding (<75% of reactivity with wild-type), except where standard error means are negligible (<2%). (a) Immunoprecipitation of the 242-282 residue mutant (exon 7) reveals that M10 is completely lost and M6 loses about 40% of reactivity by this swap. No other swaps in the middle region affected the binding of these antibodies. The 242-284 residue region in GAD65 has two hydrophilic amino acid residues, E264 and H280 and two hydrophobic amino acid residues, I253 and M258, which are not conserved in GAD67. Analysis of amino acid substitution mutants introducing the corresponding GAD67 residues into GAD65 (see Figure 1) identify E264, as essential for M10 but not M6 recognition. No effect of the other substitutions was observed. (b) Immunoprecipitation of the 308-365 residue mutant (exons 9 and 10) reveal that the M4 and b96 epitopes are lost by this swap. Analysis of 11 point mutants in this area (see Figure 1) identify a single GAD65-specific amino acid, K358, which is required for M4 but not b96 binding. No

required for conformation rather than a direct contact with the antibody. Swapping of residues 242-365 from GAD65 into the GAD67 molecule confirmed that the M6 and b96 epitopes indeed reside in this region of GAD65 (Figure 3(d)). Introduction of the critical GAD65 single amino acid residues for M10 (E264) and M4 (K358) into GAD67 was not sufficient to establish the relevant epitopes in GAD67, demonstrating that additional GAD65-specific residues confer the structural requirements for these epitopes. Interestingly, however, although M6 did not lose significant reactivity by the E264T mutation in GAD65, the reverse mutation in GAD67 (67/T273E) resulted in a partial gain of the M6 epitope (50% of wild-type GAD65 binding), confirming that this region is involved in M6 binding (results not shown).

DPC did not block any of the M1-M10 antibodies (results not shown) and did not react with the 67/242-365 chimera (Figure 3(d)), demonstrating that the DPC epitope component in residues 242-439 is outside the residues 242-365 region harboring M4, M6, M10, and b96 (Figure 3(d)). The DPC epitope mapped to the 366-413 region, which also contains the PLP-binding site of GAD65 (Figure 3(c)). This region has only three amino acid residues which are non-conserved between GAD65 and GAD67 (W379, P401, and E412) and may contribute to the conformational and/or binding requirements of the DPC epitope. The DPC epitope component in the 1-242 region mapped to the sequence P231GGS234 in exon 6 (Figure 4).

The data in Figure 4 show that the epitope of DPB mapped to residues 39-173 (mainly exons 3 and 4), and the DPD epitope and the N-terminal region component of the M8 and M9 epitopes mapped to residues 96-173 (exon 4). Because of the low degree of homology between GAD65 and GAD67, exons 3 and 4 were not amenable to homolog-scanning mutagenesis.

The data in Figure 5(a)-(f) define seven distinct epitopes in the C-terminal region of GAD65 (residues 451-585). M1/3, M7, and DPA recognize three similar but distinct epitopes, which are dependent on GAD65-specific residues in residues 483-499 and residues 556-585. N483 and H568 are essential for M7 binding, and point mutations of either of these residues significantly affect M1/3 binding, whereas only the latter seems important for DPA reactivity (Figure 5(c) and (f)). Because M1/3 and M7 do not block each other (P.S. *et al.*, unpublished results), and protect different frag-

effect of the other substitutions was observed. (c) DPC is specifically disrupted by a 366-439 swap (exons 11-13), but neither DPC nor any other middle region antibodies are disrupted by an 413-439 swap, excluding a role of GAD65-specific amino acids in exon 13 for any of the epitopes. (d) M4, M6, M10 b96, but not DPC reactivities are restored by swapping the GAD65 242-365 region into GAD67, confirming that all the middle region epitopes, except DPC, reside in this region.

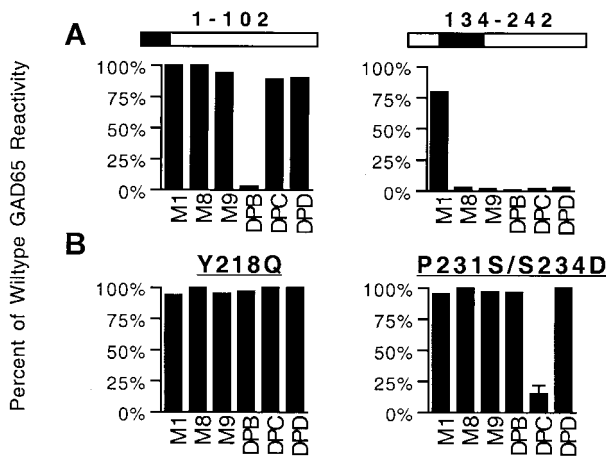


Figure 4. DPC also maps to exon 6 and DPB, DPD, M8 and M9 recognize distinct epitopes involving exon 3 and/or 4. Immunoprecipitation of [³⁵S]methionine labeled swap and point mutants in the 1-244 residue region of GAD65. The 65 and 67 regions are indicated in white and black, respectively, for each swap mutant. The results are expressed as a percentage of cpm immunoprecipitated in parallel using wild-type GAD65. The bars represent an average of three to six experiments. Error bars are shown for mutations that had a significant effect on antibody binding (<75% of reactivity with wild-type) except where standard error means are negligible (<2%). (a) DPB is the only human MAb which requires intact residues 1-102 in GAD65 for reactivity, while the M8, M9, DPB, DPC, and DPD epitopes are all disrupted by an 134-242 swap. Because DPB shows wild-type reactivity to Δ 1-8 and Δ 1-38 deletion mutants of GAD65 (data not shown) amino acid residues 39-242 in GAD65 are required for this epitope. (b) Exon 5 (residues 174-204) is conserved between GAD65 and GAD67 and the only non-conserved residues in exon 6 (residues 205-241) are a hydrophobic residue, Y218, and a cluster of neutral residues P231GG S234. Point mutations introducing GAD67 residues into GAD65, do not affect the reactivity of the DPB, DPD, M8 and M9, but identify P231 and S234 as important for the DPC epitope. This suggests that the epitopes of DPD, M8 and M9 reside in exon 4 (residues 96-173) and of DPB in residues 39-173. Furthermore, because DPC has a wild-type reactivity to a Δ 1-195 deletion mutant of GAD65, the DPC binding in residues 1-242 is likely to only involve the P231GG S234 residues in exon 6.

are essential for both M2 and M5, whereas E521, S524 and S527 are critical for M5 only (Figure 5(d)). An additional requirement for M5 but not M2 reactivity was identified within the 532-540 region of GAD65, and co-localized with b78, M8, and M9 reactivity (Figure 5(e)). A V532 K mutation specifically affected M5 and b78, probably by causing conformational changes, whereas R536 and Y540 were identified as critical binding residues for M8 and M9 only (Figure 5(e)). In addition, M8 and M9 are the only epitopes affected by the H470Q mutation (Figure 5(b)). The localization of five distinct epitopes in the 512-540 region (exon 15/16 boundary), including the N and C-terminal region epitopes (M8 and M9), suggests first that this cluster of charged residues is highly immunogenic and second, that it is in a close proximity to exon 4 in the N-terminal region. In addition to the V532 K and M523R substitution, GAD67 contains other drastic amino acid changes in the 512-540 region; for example, both E517 and E520 are proline residues in GAD67. Thus, GAD67 is expected to have a significantly different conformation in this area.

To summarize, the mapping of 14 distinct epitopes recognized by the panel of 16 human MAbs revealed that (1) two N-terminal domain restricted epitopes, DPB and DPD, reside in exons 3-4 and exon 4, respectively. (2) Of the five epitopes with middle region specificity, DPC requires GAD65-specific amino acid residues residing in exon 6 and exons 11-12 (which contain the GAD65 active site), the M4 epitope is lost by a single GAD65-specific amino acid mutation in exon 10, M10 is lost by a single amino acid mutation in exon 7, whereas b96 localizes to the same region as M4 (exons 9-10), but does not share the single amino acid requirement for reactivity, and M6, although moderately affected by swaps in exon 7, does not share the amino acid requirements of the other antibodies in this region. (3) Of the six epitopes with C-terminal specificity, M1/3, M7, and DPA recognize distinct epitopes requiring amino acids from exons 14 and 16; M2, M5, and b78 recognize an overlapping cluster of charged residues in exon 15 and/or 16. (4) The two epitopes with both N and C-terminal specificity, M8 and M9, require GAD65-specific residues in exons 4, 14, and 16. M8 and M9 are only differentiated by blocking studies (P.S. *et al.*, unpublished results).

GAD65 model structure

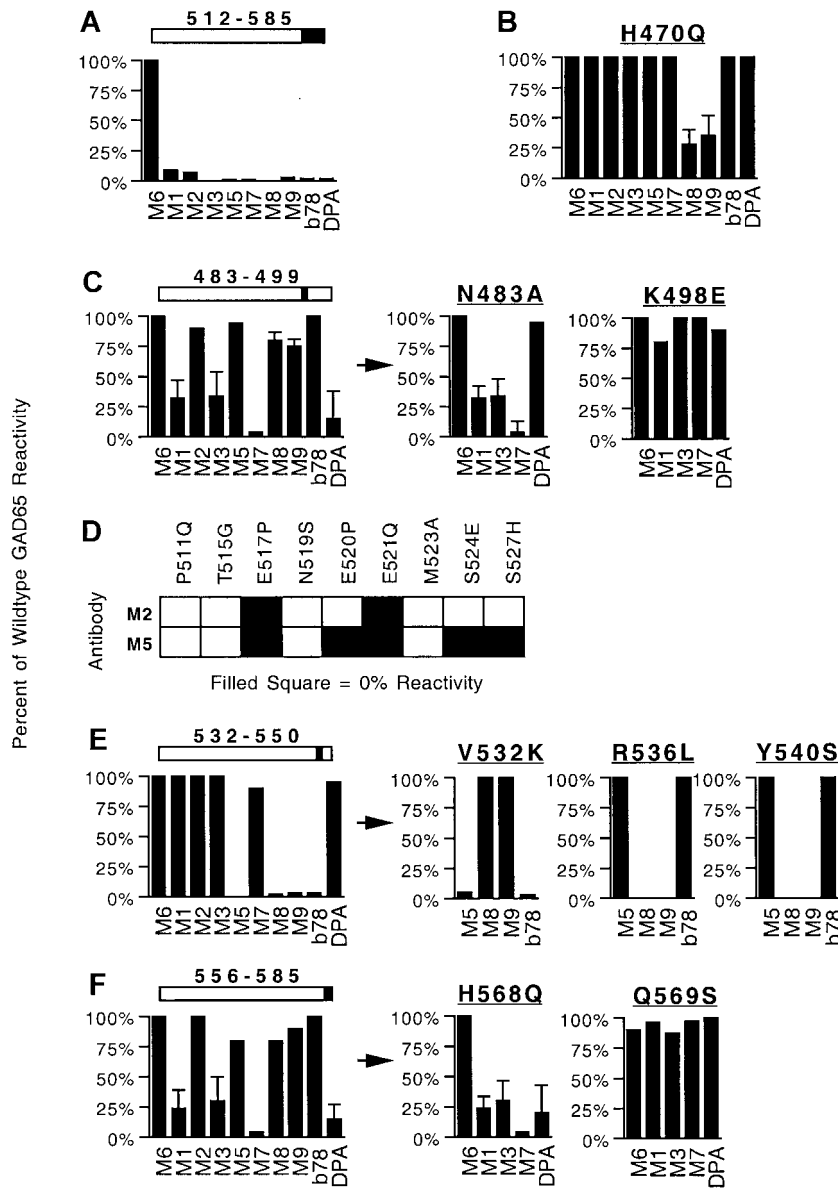
Group II decarboxylases, which include human GAD65, share a common PLP-binding motif with group III decarboxylases (Sandmeier *et al.*, 1994), including 1ORD for which a crystal structure is available (Momany *et al.*, 1995a). The TOM algorithm (Defay & Cohen, 1996), with the modifications described in the Materials and Methods, was used to generate an alignment of the PLP-binding middle region of GAD65 (residues 211-460) to 1ORD (Figure 6). Similar elements of secondary structure are readily observed between the

ments in antibody footprinting analysis (results not shown), and because DPA blocks M1/3 but not M7 (results not shown), we interpret this data to suggest that N483 and H568 may be directly involved in M7 binding and also required to maintain the correct conformation of the M1/3 (N483 and H568) and DPA (H568) epitopes. Since we have not identified GAD65-specific point mutants that result in a complete loss of M1/3 and DPA binding, it is likely that these epitopes require GAD65-specific residues for conformation while the critical antibody contact residues are shared between GAD65 and GAD67.

M2, M5, M8/M9 and b78 recognize distinct residues in the residues 512-540 region. E517 and E520

1ORD and GAD65 molecules in this region. The main differences between the two proteins in the PLP-binding domain are localized to several long loop regions, which are present in 1ORD, but are either shorter or missing in GAD65. One region predicted to contain a short helix in GAD65 (resi-

dues 258-271, helix J) is missing in 1ORD (Figure 6). This region contains the PEVKEK motif, which has significant homology to the Coxsackievirus B4 protein P2-C, and is a potential molecular mimicry epitope in GAD65 (Tian *et al.*, 1994). The M10 antibody recognizes an amino acid residue within this



D496/Q500E) only revealed an effect of the N483A mutation, which resulted in a near total loss of M7 reactivity, partly affected M1/3 binding but had no effect on DPA. (d) A large cluster of charged, non-conserved residues (residues 511-528) contains the most significant amino acid differences between GAD65 and GAD67 in the C-terminal region. Point mutants throughout this region only affect the reactivity of M2 and M5, and identify E517, and E521 as essential for both M2 and M5, and S520, S524, and S527 as essential for M5 only. (e) The 532-550 (exon 15) residue swap, which covers all hydrophilic amino acid differences between GAD65 and GAD67 in the 529-567 region disrupts the epitopes of M5, M8, M9 and b78, but no other monoclonal antibodies. Because identical results were obtained with an 532-540 residue swap, whereas an 540-550 residue swap had no effect (data not shown), a role of GAD65-specific amino acids in the latter region can be excluded. Point mutant analysis in the 532-540 region show that the M5 and b78 epitopes are specifically disrupted by a V532 K mutation, and identify R536 and Y540 as essential residues for M8 and M9. (f) Immunoprecipitation analysis of the 556-585 residue swap reveals that the M7 epitope is lost by this mutation and that M1/M3 and DPA are significantly affected. This region contains only two amino acid differences between GAD65 and GAD67 (H568Q and Q569S). The corresponding point mutants reveal that H568 is essential for M7, and that the H568Q mutation partly affects the M1/M3 and DPA reactivities. In contrast, a Q569S mutation leaves the epitopes intact.

Figure 5. Fine mapping of the C-terminal region epitopes, M1, 2, 5, 7, 8, 9, b78, and DPA. Immunoprecipitation of [³⁵S]methionine labeled swap and point mutants in the C-terminal domain of GAD65. The 65 and 67 regions are indicated in white and black, respectively, for each swap mutant. The results are expressed as a percentage of cpm immunoprecipitated in parallel using wild-type GAD65. The bars represent an average of three to six experiments. Error bars are shown for mutations that had a significant effect on antibody binding (<75% of reactivity with wild-type), except where standard error means are negligible (<2%). (a) All C-terminal reactive human Mabs require intact 512-585 residues in GAD65. Complementary large swaps (residues 451-512 and 446-525) were unstable and could not be expressed at sufficient levels for immunoprecipitation analysis. Small chimeric proteins and point mutants were therefore used for further dissection of the C-terminal region. (b) The region between residues 440 and 482 contains three hydrophilic residues which are not conserved in GAD67. Analysis of the corresponding amino acid mutations (T465V, H470Q, and D472N) only revealed an effect of the H470Q mutation on M8 and M9. (c) Analysis of an adjacent swap (residues 483-499), which contains four polar non-conserved residues, results in a near total loss of M7 reactivity and a significant reduction in DPA and M1/3 binding. Analysis of four point mutants in or adjacent to this region (N483A, I484 K, K498E, and

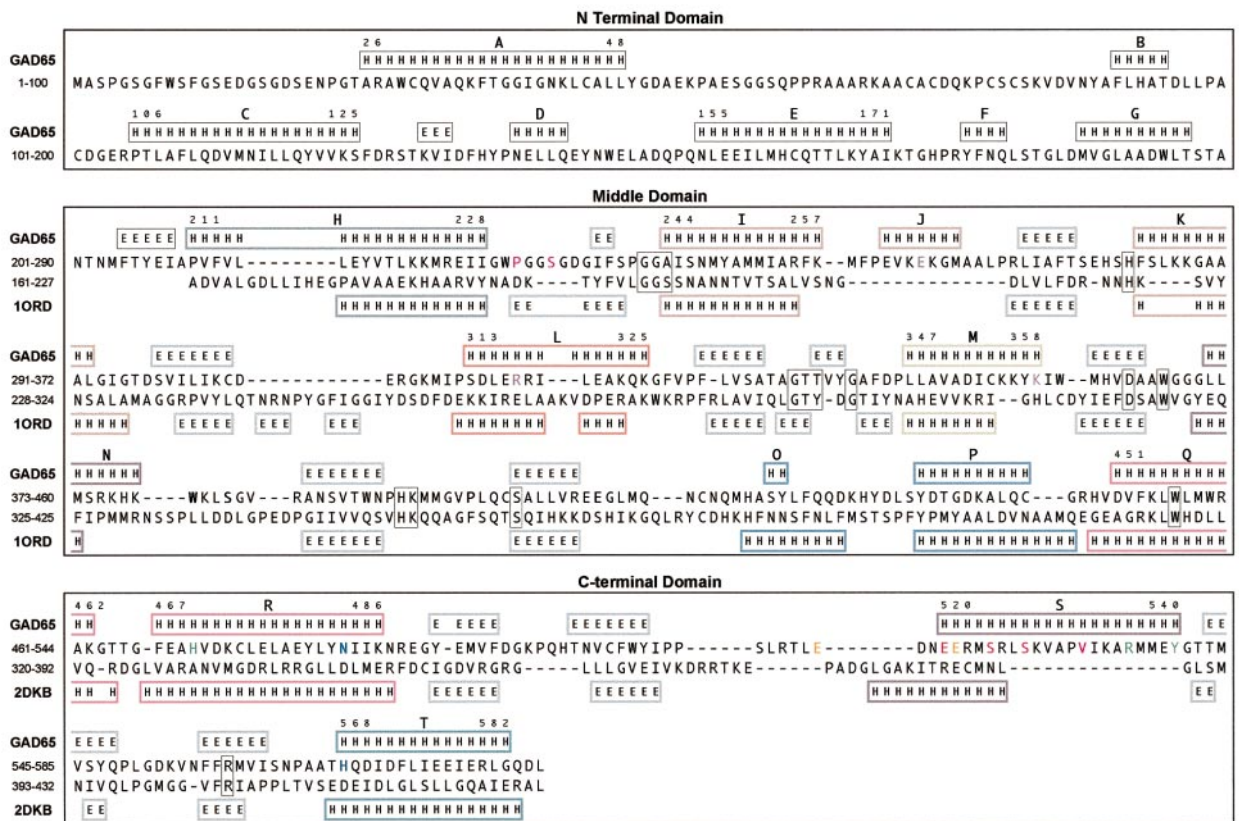


Figure 6. Secondary structure prediction and threading of GAD65. The sequence of the middle and C-terminal domain of GAD65 was threaded onto the PLP-binding domain of 1ORD (ORD residues 161-425/GAD65 residues 211-460) and the C-terminal domain of 2DKB (DKB residues 320-432/GAD65 residues 461-585) using a modified TOM algorithm (Defay & Cohen 1996). Secondary structure predictions (for GAD65) and PDB assignments (for 1ORD and 2DKB) are indicated by boxes of Hs (α -helices) and Es (β -strand) above or below the sequence. GAD65 and ORD differ mainly in the PLP-binding domain by several loop regions present in ORD but either missing or shorter in GAD65. One region (residues 258-271 in GAD65) containing helix J is missing in 1ORD. In the C-terminal region, the main difference between GAD65 and 2DKB is the length of the second α -helix (S), which is longer in GAD65. Amino acid residues affecting Mab recognition are shown in color. Boxed amino acids correspond to conserved residues between decarboxylases, which are likely to be functionally important and which served as "anchors" in the alignment.

motif (E264), providing the first evidence that this region is recognized by type 1 diabetic sera. However, M10 does not recognize the P2-C protein (data not shown), demonstrating that the linear homology region in P2-C does not acquire a conformation similar to that of GAD65.

To identify a structural homolog for the C-terminal region (residues 461-585) of hGAD65, the TOM algorithm was used to search a library of known structural folds (Defay & Cohen, 1996) using the predicted hGAD65 secondary structure. This search identified a member of the group I decarboxylases, dialkylglycine decarboxylase (2DKB). Alignment of the C-terminal regions of hGAD65 and 2DKB suggested significant structural homology between the molecules, with the major difference being the length of the second helix in the region which is significantly extended in hGAD65 (residues 517-540; Figure 6).

In the absence of protein(s) of known structure with significant homology to the N-terminal domain of GAD65, the secondary structure of this

region was predicted using the algorithm by Chandonia & Karplus (1999) (Figure 6).

Native GAD65 has been shown to form a non-covalently associated dimer (Sheikh & Martin 1996 and results not shown). A three-dimensional model of the middle and C-terminal regions of GAD65 was built and modified as described in the Materials and Methods, using the 1ORD and 2DKB templates. The information obtained from the epitope studies was used to refine the model so that amino acid residues in the same epitope were spatially close, with side-chains involved in antibody binding pointing toward the same face of the protein. The resulting model is shown in Figures 7-9.

The M4, M6, M10 and b96 middle region epitopes co-localize to a charged patch, while the DPC epitope localizes across the PLP-binding pocket

Figure 7 shows a model of the three-dimensional structure of the middle domain of a dimer of

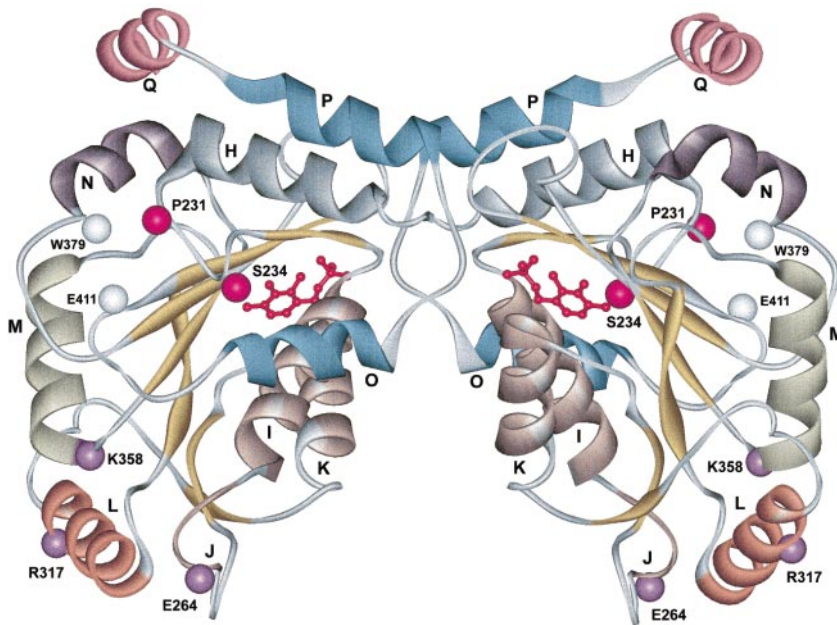


Figure 7. Three-dimensional model of the middle region of a GAD65 dimer. Two monomers of GAD65 (related by P_{21} -symmetry) are shown. The lettering of α -helices and the coloring of α -helices and β -strands are as described in the legend to Figure 6. PLP molecules are modeled (in red) in the PLP-binding pocket, which is highly similar to that of 1ORD. Helix J in the PEVKEK region is predicted to be a loose open helix or a loop. This region contains E264 (purple) which is essential for M10 binding and involved in M6 binding. K358 shown in purple at the C-terminal end of helix M is essential for the M4 epitope. R317 shown in purple in helix L is essential for several GAD65-specific mouse monoclonal antibodies which map to the same region as M4 and b96 (residues 308-365) and

yet block M10 more efficiently than M4. The two GAD65-specific amino acids in exon 6 involved in the DPC epitope (P231, S234) are shown in pink. The two adjacent GAD65-specific amino acid residues which differ significantly between GAD65 and GAD67 in the exon 11-12 component of the DPC epitope, W379 and E411, are shown in white.

GAD65. The PLP-binding middle region consists of a seven-stranded β sheet surrounded by seven helices. E264, which is involved in the M10 and M6 epitopes, points upwards in this model away from the β -sheet and the PLP-binding pocket and forms a small charged patch together with K358, which is essential for M4 binding and resides adjacent to the C-terminal end of helix M (residues 348-356), and R317 on helix L (residues 313-324), which is a critical residue for the epitope(s) of two GAD65-specific monoclonal mouse antibodies, which localize to this region (H.L.S., F. Luhder & S.B., unpublished results). The co-localization of these critical amino acids to the same hydrophilic patch is consistent with the ability of the M4, M6 and M10 antibodies to block each other (P.S. *et al.*, unpublished results) and suggests that this region of GAD65 is highly immunogenic.

Exons 11 and 12, which are implicated in the DPC epitope (Figure 3(c)) contain three non-conserved amino acid changes between GAD65 and GAD67. Two of these, W379 and E412, flank the active site of GAD65 and localize near P231 and S234 adjacent to the H helix (residues 211-228) in exon 6, which were identified as important for DPC binding. P401 can be excluded because it resides in a loop region on the opposite face of the PLP-binding pocket away from S231 and S234. Thus, the DPC epitope rests at the back of the PLP-binding pocket, away from the active site, consistent with its inability to inhibit GAD65 enzymatic activity (results not shown).

The C-terminal and middle domains of GAD65 are connected by helix Q (residues 451-461) which

is conserved in GAD65, GAD67, and 1ORD (Figures 7-9).

C-terminal epitopes cluster on three charged helices

The three-dimensional model of GAD65 in the C-terminal region predicts an α/β fold composed of a four-stranded β -sheet and three amphipathic α -helices (Figure 8), with localization of hydrophobic residues towards the β -strands and residues involved in epitope recognition on the charged face of these helices (Figure 8). Helix S (residues 521-540) contains charged amino acid residues identified for M2, M5, M8, and M9 binding (Figure 5), which are separated by four amino acids; this is consistent with these residues forming a charged face of an α -helix. The amino acid residues identified for M8 and M9 reside at the C-terminal end of helix S. The H470 residue in the hydrophobic face of helix R is not predicted to be in a direct contact with M8 and M9 binding because the H470Q mutation, which may affect stacking of helices and β -strands in the epitope area, decreases rather than abolishes binding. Helices R and T contain the N483 and H568 residues identified as critical for M7 binding (Figure 5). M1/3 and DPA are also affected by swaps and point mutations on helices R and T, but they constitute a separate blocking group and may be dependent on GAD65-specific residues in this region for conformation rather than for direct contact. Based on spatial considerations, their epitopes are most likely located along the charged face of

the R helix (E468, D472, E479, K486), 5-7 Å away from N483, which they do not block.

Human autoreactive MABs recognize epitopes on the surface and define multiple autoreactive regions in the native GAD65 molecule

The predicted C-terminal and middle domains of GAD65 were aligned using the connecting helix (residues 451-461) and R558 (Figure 9). Antibody blocking data were used to refine a space-filling

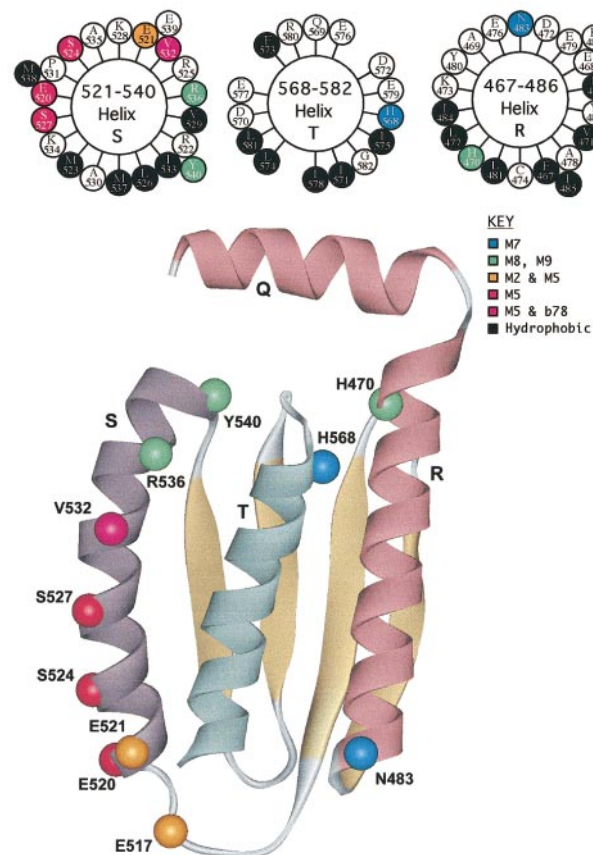


Figure 8. Helix wheel projections and a three-dimensional model of the C-terminal domain of a GAD65 monomer. Helix wheel projection viewed from the N-terminal end of the three α -helices in the C-terminal region of GAD65, reveal amphipathicity and clustering of epitopes on the hydrophilic faces of the helices. The lettering of α -helices and the coloring of α -helices and β -strands are as described in the legend to Figure 6. Hydrophobic amino acid residues, shown in black, localize towards the β -sheet. E517 and E520 at the N-terminal end of helix S are critical residues for the only linear epitope M2. These same residues, together with S524 and S527, are critical for M5 binding. The V532 K mutation completely disrupts both M5 and b78. R536 and Y540 are essential residues for M8 and M9. H470, which is also implicated in the M8 and M9 epitope, is in the hydrophobic face of helix R and the H470Q mutation may affect stacking of helices/ β -sheets in the M8/M9 epitope area. N483 and H568 are critical for M7 binding. Mutation of those residues may affect the conformation of M1/M3 and DPA.

model and to rule out orientations which were spatially inconsistent with the blocking groups. The composite model shown in Figure 9 indicates the spatial localization of the identified epitopes, which cover almost the entire surface of GAD65.

The N-terminal region is predicted to bind across the top of the P helix in the middle region, in an orientation similar to that of 1ORD (Momany *et al.*, 1995a), providing hydrophobic regions to cover several otherwise exposed hydrophobic residues in helix P. Exon 4, which is implicated in the DPB, DPD, M8 and M9 epitopes, contains two long amphipathic α -helices (Figure 1). The N-terminal component of the M8 and M9 epitopes is likely to reside in the hydrophilic face of one of these helices and be located adjacent to the C terminus of helix S in the native GAD65 molecule to form these epitopes.

Discussion

This study presents the biochemical and structural mapping of 13 distinct conformation-dependent and one conformation-independent humoral epitopes in the β -cell autoantigen glutamate decarboxylase 65 (GAD65). The mapping of amino acid residues involved in distinct conformational epitopes has been used together with two and three-dimensional structure prediction methods to generate a model of the GAD65 dimer. It should be emphasized that the structural model presented here must be interpreted with caution. Although the choice of template structures (1ORD and 2DKB) is likely to be correct due to their identification both by the modified TOM algorithm and by the PSI-BLAST program (see Materials and Methods) the very low level of sequence homology makes some details of the alignment uncertain. Register shifts of several residues in the alignment are likely, especially in positions far removed in sequence from the "anchor" residues. Loop regions in which insertions or deletions occur in the template sequences are especially prone to errors in backbone conformation (Sali & Blundell, 1993). However, the current model does provide a useful context in which to interpret experimental data until it is possible to determine the structure experimentally.

The epitopes are defined by 16 human monoclonal antibodies derived from four type 1 diabetic patients, and one islet cell antibody positive individual with polyendocrine autoimmunity syndrome. The autoreactive epitopes, including the linear epitope, map to hydrophilic patches exposed on the surface of the folded GAD65 molecule. The epitopes cluster to distinct areas: a hydrophilic patch in the middle region defined by the M4, M6, M10 and b98 blocking groups, the S-helix in the C-terminal region where M2, M5, b78, M8 and M9 bind, and exon 4 in the N-terminal region where DPB, DPD, M8 and M9 bind. However, epitopes within each cluster can clearly be distinguished by

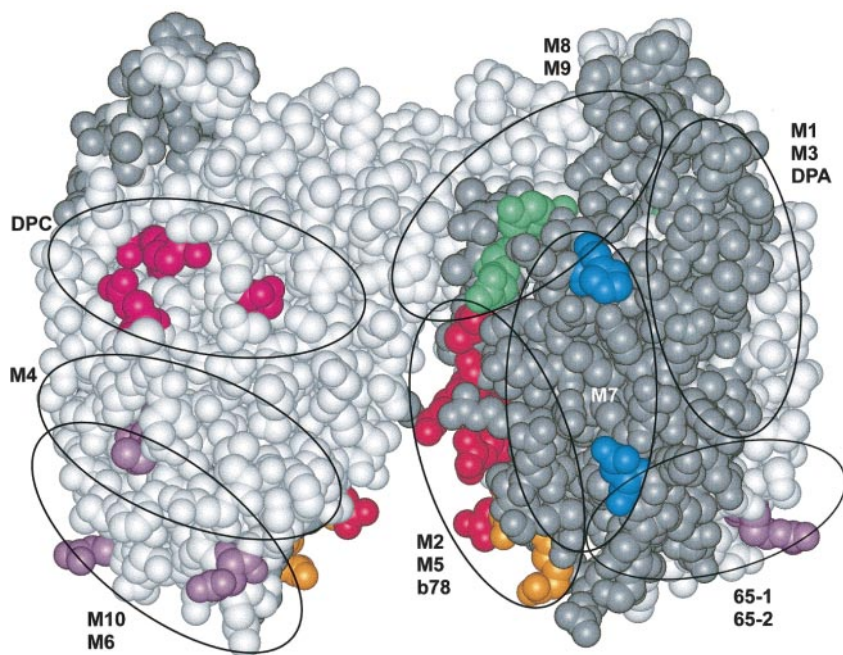


Figure 9. Space-filling model of GAD65. To orient the predicted C-terminal and middle domains of GAD65, two homologous regions were used. First, the connecting helix (helix Q, residues 451-461) which is conserved between GAD, 1ORD, and 2DKB, was used to manually align the two domains. This localizes the C-terminal domain (gray) directly on top of the PLP-binding pocket in the middle domain (white). Second, the conserved R558 residue in GAD65 and 2DKB was manually aligned to interact with the PLP pocket in a manner similar to both the 2DKB and amino acid transferase structures (Toney *et al.*, 1995). Thus the exposed backside of the PLP-binding region containing the hydrophobic β -sheet is covered with the hydrophobic face of the β -sheet and α -helices in the C-terminal region. Approximate locations of

Mab recognition are colored corresponding to Figures 68. Antibody blocking groups are indicated by overlapping circles. From the top, M8 and M9 (green) bind directly across from DPC (pink) at a similar topological location on the opposing face on the dimer. Similarly, the C-terminal epitopes (blue, red, orange) cluster on equivalent locations to the middle region epitopes (purple) on the opposing side of the dimer. Within the C-terminal epitopes, M7 (blue) binds across the face of two helices (helices R and T) forming a blocking group with M8 and M9 (green), as well as, M2, M5, and b78 (orange, red) which bind to an exposed helix (helix S) near the dimer interface. M1, M3, and DPA are predicted to bind the backside of helix R and possibly to conserved residues in the middle domain. Two murine monoclonal antibodies, 65-1 and 65-2, which block M7 but not M1/3, bind the bottom region of the dimer and span both the C-terminal and middle domains, wrapping around the side of the dimer and forming a blocking group with M10. The N-terminal domain of GAD65 is predicted to be located at the top of this model in an orientation similar to that of 1ORD (Momany *et al.*, 1995a).

different anchor residues and boundaries. Furthermore, the autoreactivity is not restricted to these regions of GAD65. Rather, the target epitopes of the human monoclonal antibodies cover almost the entire surface of GAD65 and reveal a remarkable degree of autoreactivity in all three domains of the protein. With the exception of the DPC epitope, all the autoreactive epitopes map to regions of the molecule which are targeted by monoclonal antibodies derived from two or three patients, demonstrating that they are not limited to one individual.

All the monoclonal antibodies are specific for GAD65 and do not recognize a second glutamate decarboxylase isoform, GAD67, which shares a 76% identity with GAD65 in the middle and C-terminal domain (Bu & Tobin, 1994). Of the 23 GAD65/67 domain and exon swap mutants and 37 GAD65 point mutants generated for this study, five did not express at detectable levels, suggesting instability during expression. All other mutants expressed at levels comparable to wild-type, and their integrity could be monitored by antibodies recognizing conformational GAD65 epitopes residing outside the mutated area. Several of those mutants were conformationally stable during short incubations, but unfolded and lost epitopes in regions outside the mutated area during overnight

incubations or upon freezing and thawing, demonstrating that the use of freshly made protein, short incubations and conformational controls in binding experiments is crucial for the epitope studies. Amongst the 37 GAD65/67 point mutants, however, only two did not express, and only one unfolded during overnight incubations. In the fine mapping of the human autoreactive epitopes using the point mutants, we have assumed that a complete loss of antibody binding by a point mutation in a hydrophilic residue indicates that this residue is involved in binding of the antibody, whereas a partial effect of a mutation of a hydrophilic amino acid or any effect of a hydrophobic amino acid mutation are likely to be caused by a conformational change (Cunningham *et al.*, 1989 and references therein). By this criteria, we were able to identify the GAD65-specific amino acids which are involved in binding of eight of the antibodies (M2, M4, M5, M7, M8, M9, M10, and DPC), whereas five epitopes (for antibodies M1/3, M6, b78, b96, DPA) were defined by small conformational changes caused by GAD65/67 substitutions rather than by complete loss of an epitope. This suggests that for some of the epitopes the critical binding residues are conserved between GAD65 and GAD67, whereas GAD65-specific residues are

essential for maintaining the correct epitope conformation. Further identification of amino acid residues that bind the latter group of antibodies will require alanine walking of conserved GAD65 residues in the epitope regions.

Finally, two of the antibodies, DPB and DPD, are entirely dependent on amino acids in an area of GAD65 which has little homology to GAD67 (exons 3 and/or 4), or to any proteins whose crystal structure has been solved. This region was therefore less tractable for study by homolog-scanning mutagenesis and not appropriate for homology-based molecular modelling. Nevertheless, because these antibodies only bind to the native GAD65, the corresponding epitopes must also reside on the surface of the folded protein. Two predicted long amphiphilic helical regions in exon 4 represent candidate areas for epitopes in this region.

In type 1 diabetes, 95% of GAD65 autoantibody positive sera only recognize conformational epitopes in the native molecule. In this respect, the human monoclonal antibodies are representative of diabetic sera. Many of the autoreactive epitopes/regions defined here also seem to represent epitopes generally recognized by type 1 diabetic patients (H.L.S., & S.B. unpublished results).

Interestingly, none of the monoclonal antibodies target the first two exons in GAD65. These exons may be buried in the folded molecule, since rabbit antisera raised to peptides in this region only recognize the protein under partially denaturing conditions (results not shown). Development of antibodies to a linear epitope residing in the first eight amino acid residues of GAD65 is a characteristic of stiff-man syndrome and distinguishes it from type 1 diabetes (Kim *et al.*, 1994). We infer that exposure of this peptide would require unfolding and/or degradation of GAD65. Four of the monoclonals recognize amino acids in exon 3 and/or 4 in the N-terminal region. The region around residues 69-70 in exon 3, is a proteolytic hot spot in native GAD65 (Christgau *et al.*, 1992; Kim *et al.*, 1994) and may therefore be exposed on the surface of the unfolded protein.

Several T-cell epitopes have been defined for one of the HLA-susceptibility haplotypes for type 1 diabetes, HLA-DRB1 *0401 (Endl *et al.*, 1997; Patel *et al.*, 1997; Wicker *et al.*, 1996). Interestingly, the dominant T-cell epitopes for this haplotype reside adjacent to or in regions harboring autoimmune B-cell epitopes. For example, M6 and M10 require residues 242-282 in GAD65 for binding, and this portion of the molecule also harbors dominant T-cell epitope(s) for 0401 (Endl *et al.*, 1997; Patel *et al.*, 1997; Wicker *et al.*, 1996). Similarly, residues 483 and H568 are critical residues for M7, and reside in or adjacent to dominant T-cell epitopes in residues 481-499 and 551-565 (Patel *et al.*, 1997). Interestingly, M7 protects a distinct small peptide in footprinting experiments (H.L.S. & S.B., unpublished results). M2 and M5 also bind residues in the midst of a subdominant T-cell epitope (residues

511-525; Patel *et al.*, 1997). The N-terminal region of exon 4, which is important for the DPB, DPD, M8 and M9 epitopes, also contains a T-cell epitope in residues 116-130 (Patel *et al.*, 1997). Thus, for the DRB1 *0401 allele, B and T-cell epitopes seem to cluster in the same regions of the protein. The antibody specificity of a B-cell can influence which epitopes it presents to a T-cell (Simitsek *et al.*, 1995). Surface-bound Ig, may either: (1) enhance the presentation of a T-cell epitope within its binding region by protecting it from proteolysis that would otherwise destroy it; or (2) prevent its presentation by remaining associated with it too long during endocytosis, proteolytic processing, and MHC-class II antigen loading. Similarly, antibody specificity could exert an effect on processing and presentation of antigen taken up as an immune complex by a macrophage. With regard to GAD65, the co-localization of B and T-cell epitopes for at least one susceptibility haplotype suggests that autoreactive Ig molecules may enhance the presentation of T-cell epitopes in their binding region.

How does an intracellular molecule like GAD65 become presented to autoimmune B-cells in its native form? If GAD65 was only presented to the immune system following destruction or apoptosis of pancreatic β -cells and consequent protein degradation, development of antibodies to linear epitopes and to epitopes masked in the native structure would seem likely, because there is no indication that the protein is particularly resistant to proteolysis (results not shown). However, in contrast to autoantibodies to myelin basic protein in multiple sclerosis, which predominantly target a linear epitope (Wucherpfennig *et al.*, 1997) buried in the native molecule (Ridsdale *et al.*, 1997), GAD65 autoantibodies in type 1 diabetes are almost entirely restricted to conformational epitopes residing on the surface of the folded molecule. Is it possible that native GAD65, or perhaps GAD65 cleaved at a proteolytic hot spot at residues 69-70, can be secreted from the β -cell? GAD65 is synthesized in the cytosol but becomes anchored to the cytosolic face of small synaptic vesicles in pancreatic β -cells and synaptic vesicles in neurons (data not shown). These vesicles accumulate its product GABA for exocytosis. Because GAD65 localizes to the cytosolic face of synaptic vesicles (L.-A. Lindsay & S.B., unpublished results) it is expected to localize briefly to the cytosolic rather than outer face of the plasmalemma during exocytosis. The nature of the autoreactive antibodies invokes a mechanism by which GAD65 can translocate to the surface and leave the cell before endocytosis brings it back to synaptic vesicles.

The autoreactivity to GAD65 in human patient sera is clearly not restricted to a single region, which might be envisioned to result from a molecular mimicry by an immunogenic epitope carried by an infectious agent. Rather, the whole surface of the protein is covered with autoreactive epitopes. In contrast, the GAD67 isoform, which is highly homologous in most of the epitope areas and is

predicted to have a similar three-dimensional structure in the middle and C-terminal regions, does not share this profound autoreactivity. This difference is not easily explained by structural details of the protein backbone, or by differences in induction of immune tolerance. Rather, we propose that the autoimmunity toward GAD65 may be a consequence of its cellular localization, involving dynamic membrane anchoring, trafficking between cytosol and membrane compartments, and perhaps secretion.

Materials and Methods

Antibodies

The human monoclonal antibodies used in this study were derived from islet cell antibody positive patients and have been described elsewhere (Madec *et al.*, 1996; Richter *et al.*, 1993; Syren *et al.*, 1996; Tremble *et al.*, 1997). Normal human serum was used as a negative control antibody in all immunoprecipitation experiments. A GAD65-specific mouse monoclonal antibody, GAD6 (Chang & Gottlieb, 1988), which recognizes a linear epitope in the C-terminal region of GAD65 (and is therefore independent of conformation) was used to monitor expression levels of all GAD65 mutants, except those which eliminated GAD65-specific amino acids required for this epitope (data not shown). A second mouse monoclonal antibody, GAD1 (Chang & Gottlieb, 1988), which recognizes a shared conformational epitope between GAD65 and GAD67 (unpublished results), was used as a control for conformational stability of GAD67 and GAD65/67 chimeras. Human Mab M1, which binds an epitope in the C-terminal region (Richter *et al.*, 1993) was used as a control with middle and N-terminal region mutants to monitor the conformational stability of the C-terminal region and absence of global unfolding in areas outside the mutated area. Similarly, M6, which recognizes an epitope in the middle region (Richter *et al.*, 1993), was used as a control for conformational stability of N and C-terminal region mutants.

GAD65 and GAD67 mutants

Full-length cDNAs for either human GAD65 or GAD67 were utilized to generate chimeric constructs in the Bluescript KS-vector (Stratagene, Cambridge, MA). Constructs were generated by three strategies: (1) a unique restriction enzyme site, corresponding to the homologous sequence of GAD67, was introduced into GAD65 by site-directed mutagenesis using the method described (Kunkel *et al.*, 1987). These included *XcmI* at residue 133 in GAD65 which also resulted in a conserved I133L mutation; *XcaI* at residue 413; *Bsu36I* at residue 439; and *PmlI* at residue 451. The corresponding GAD67 region was subcloned into the mutated GAD65 cDNA to generate the final chimeric construct. (2) A mutant oligo nucleotide containing the selected GAD67 sequence was used to introduce multiple amino acid substitutions within the homologous GAD65 region by site-directed mutagenesis (Kunkel *et al.*, 1987). (3) An asymmetric polymerase chain reaction (PCR)-based strategy was used to generate some GAD65/GAD67 chimeras (Perrin & Gilliland, 1990). Using oligonucleotide primers which span the desired GAD65/GAD67 junction, an asymmetric amplification reaction was performed using the

GAD67 cDNA to generate a primarily single-stranded fragment which contains the GAD67 sequences to be swapped flanked by the GAD65 sequences from the primer. The product in this reaction was used as a primer in a second amplification reaction with the GAD65 template and an external GAD65 primer. After two separate reactions to incorporate GAD65 sequences both upstream and downstream of the GAD67 sequences, the products were mixed and amplified to give a final product containing GAD65 sequences surrounding the GAD67 domain. Finally, this fragment was subcloned back into GAD65 to yield the completed chimeric construct. For GAD65/67 point mutations, restriction enzyme sites, which provided a diagnostic pattern for screening, were either introduced or removed by site-directed mutagenesis. All constructs were confirmed by both sequencing and restriction enzyme digestion and were subcloned into the pSV-Sport expression vector (Gibco/BRL, Gaithersburg, MD). The GAD65/67 constructs generated for this study are shown in Figure 1.

The generation of deletion mutants lacking the first 8, 38 or 195 amino acid residues of GAD65 was as described (Richter *et al.*, 1993; Shi *et al.*, 1994).

Protein expression and quality

Wild-type and mutant GAD65 and GAD67 proteins were expressed from the corresponding cDNA by *in vitro* transcription/translation using the TNT SP6 Coupled Reticulocyte Lysate System (Promega, Madison, WI) in the presence of [³⁵S]methionine (≥ 1000 Ci/mmol, Amersham, Arlington Heights, IL). Unbound radioactivity was removed by gel filtration of the transcription/translation mixture on a PD10 column, containing Sephadex G-25 (Pharmacia, Uppsala, Sweden) in immunoprecipitation buffer (10 mM Hepes, 10 mM benzamidine/HCl, 150 mM NaCl, 0.5 mM methionine, 5 mM EDTA, 0.1% (w/v) bovine serum albumin, and 0.5% (v/v) Triton X-114; IP buffer).

The proteins generated by the *in vitro* system were full-length as determined by SDS-PAGE analyses before and after immunoprecipitation with GAD6. In pilot experiments [³⁵S]methionine labeled swap mutants (242-282, 242-308, 242-439, 308-365, 366-439, 451-585) were produced either in a COS-7 cell expression system (Richter *et al.*, 1993) or in the *in vitro* transcription/translation system and used in immunoprecipitation binding assays (see below) with the MICA antibodies. The experiments yielded identical results with protein produced in the two systems, demonstrating that the conformational quality of the *in vitro* produced protein is similar to that of the protein in COS cells. The *in vitro* material was used in all subsequent assays. In each experiment, the *in vitro* generated material was analyzed with several conformation dependent control antibodies in order to monitor the stability of the mutant and the conformational integrity of regions outside the mutated area. All proteins were freshly prepared for each immunoprecipitation experiment because some chimeras became unstable during a prolonged incubation (>12 hours) at 4°C and/or upon freezing and thawing.

Immunoprecipitation

All procedures were performed at 4°C. Aliquots containing 50,000 cpm of freshly labeled wild-type or mutant proteins in 100 μ l of IP buffer were incubated for a minimum of two hours with antibody in either Eppen-

dorf tubes or 96-well microtiter plates (Millipore Multi-screen Assay, Millipore, Bedford, MA). Antibodies were diluted in IP buffer or used undiluted at a concentration that yielded between 3000 and 5000 cpm in pilot immunoprecipitation experiments with wild-type protein. All volumes were kept identical within each experiment. Immunocomplexes were isolated by adsorption to 20 μ l of a 50% slurry of Protein A-Sepharose (Pharmacia) in IP buffer for 45 minutes at 4°C. The Sepharose beads were washed five times in IP buffer to remove unbound protein. Immune complexes isolated in Eppendorff tubes were eluted by boiling in an SDS-sample buffer (Laemmli, 1970), followed by scintillation counting using Ecolume (ICN, Costa Mesa, CA). The samples in microtiter wells were analyzed by scintillation counting as described (Petersen *et al.*, 1994). The two methods gave similar results. Normal human serum (5 μ l) was used as a negative control in all immunoprecipitation experiments. In each analysis of antibody reactivity to a mutant, wild-type GAD65 was immunoprecipitated in parallel. The wild-type cpm minus cpm obtained with normal human serum were assigned a value of 100%. Results for the mutants were expressed as a percentage of the value for wild-type. Analysis of each mutant was repeated a minimum of three times. For mutants which had a partial effect on antibody binding, the analyses were repeated five to six times.

Protein footprinting and antibody blocking

Immune complexes were prepared using *in vitro* translated [³⁵S]methionine, [³⁵S]cysteine (≥ 1000 Ci/mmol, Amersham), or [¹⁴C]leucine (300 mCi/mmol) labeled GAD65 and antibodies and washed as described above. To stabilize the immune complexes, goat-anti-human IgG antibody (heavy and light-chain-specific F(ab')₂ fragments; Jackson ImmunoResearch, West Grove, PA) was incubated with the antigen-antibody-PAS complex for 45 minutes at 4°C for 30 minutes to stabilize the immune complex, followed by two washes in trypsinization buffer (10 mM Hepes, 150 mM NaCl). Incubation with trypsin (2 mg/ml; Sigma, St. Lois, MS) was at 37°C for 90 minutes. Protease treatment was stopped by washing the PAS-bound complexes in IP buffer. Ig associated fragments were eluted in Tris/tricine sample buffer and analyzed by Tris/tricine gel electrophoresis (Schagger & von Jagow, 1987) followed by autoradiography for seven to 45 days. Only the M1-M10 antibodies, which were available in sufficient quantities, were used for these analysis.

Antibody blocking studies were carried out as described (Syren *et al.*, 1996).

Sequence alignment algorithms used for molecular modeling

To determine the three-dimensional localization of the epitopes defined in this study, a profile of aligned sequences with >30% identity to full-length human GAD65 was generated using the CLUSTALW program (Thompson *et al.*, 1994) and used to predict the secondary structure of GAD65 using the algorithm of (Chandonia & Karplus, 1999). Sequences were obtained from GenBank and included: human GAD65, Q05329; human GAD67, Q99259; porcine GAD65, P48321; porcine GAD67, P48319; mouse GAD65, P48320; mouse GAD67, P48318; rat GAD65, Q05329; rat GAD67, P18088; feline GAD65, P14748; *Drosophila* GAD1, P20228; *Drosophila* GAD2, U01239; rat cysteine sulfinate decar-

boxylase, X94152; and xenopus GAD, U38225. Typically, proteins with 15-25% sequence identity share a common tertiary fold, but it is frequently difficult to identify the correct alignment (Taylor, 1989). Profiling or threading algorithms have improved this situation somewhat (Dunbrack *et al.*, 1997). It is in this context that reliable models of the structure of GAD65 were sought.

Alignment of the GAD65 sequence to three dimensional templates was performed using a version of the TOM threading algorithm (Defay & Cohen, 1996) which was modified to include information on predicted secondary structure. TOM uses a dynamic programming algorithm (Falicov & Cohen, 1996) to calculate an alignment (including gaps) between the template and model sequences which optimizes a scoring function. This scoring function is derived from data on multiple sequences homologous to the model protein, and largely reflects the tendency of various positions to be buried in the protein core or exposed to solvent.

The Pred2ary secondary structure prediction algorithm (Chandonia & Karplus, 1999) predicts the probability of helix, strand or coil occurring at each position in the sequence. For soluble, globular proteins, the highest of the three probabilities corresponds to the correct secondary structure with an average accuracy of over 75%; either the first or second alternative is correct at 94% of the positions (Chandonia & Karplus, 1999). The predicted secondary structure probabilities were used to calculate the expected distribution of backbone dihedral angles for each residue in the sequence. These distributions were translated into an energy potential using the quasichemical approximation (Miyazawa & Jernigan, 1985), and the potential was used as a scoring function in combination with the original TOM (Defay & Cohen, 1996) scoring function. Both scoring functions were weighted equally.

A version of the TOM program which used the new scoring function was tested on a set of 58 proteins used in previous threading tests (Defay & Cohen, 1996). The program was used to align each sequence with the structures of one or more remote homolog (proteins having <25% sequence identity, but similar core tertiary structures). Alignments were compared to the correct alignments, which were obtained using a structural comparison algorithm (Falicov & Cohen, 1996). Relative to the original TOM program, average alignment accuracy improved from 38% to 52% of residues placed within one position of the correct alignment (J.M.C. & F.E.C., unpublished results).

Alignment of the GAD65 sequence with the 1ORD and 2DKB folds described below is expected to be significantly more accurate due to the additional information available for this molecule, i.e. location of conformational epitopes and conservation of residues, considered to be part of the PLP binding site, between 1ORD and GAD65 (see below). These conserved residues serve as anchors, which prevent large shifts in the predicted alignment with 1ORD. Because these positions are distributed throughout the middle region of the GAD65 sequence, errors in the alignment should be substantially reduced relative to errors on the 58 test proteins.

Molecular modeling of GAD65

The PLP binding region of ornithine decarboxylase (1ORD) was selected as a template for modeling the PLP-binding region of hGAD65 due to the conservation of several residues between 1ORD and GAD65 in this

region, which are considered to be important for PLP binding (see below). The structure of 1ORD has been determined by X-ray crystallography at 3.0 Å resolution (Momany *et al.*, 1995a). The improved TOM algorithm revealed significant similarities between folds in the C-terminal region of GAD65 and the C-terminal domain of dialkylglycine decarboxylase (2DKB). The structure of 2DKB has been determined by X-ray crystallography to a resolution of 2.1 Å (Toney *et al.*, 1995), and was selected as a template for threading and three-dimensional modeling of the C-terminal region of GAD65. The homology to the templates in both the middle and C-terminal regions of GAD65 was further supported by results from the PSI-BLAST program (Altschul *et al.*, 1997), which identified both 1ORD and 2DKB as possible homologs of hGAD65. PSI-BLAST was used to create a position-specific substitution matrix using the hGAD65 sequence and the non-redundant sequence database, which was then used to search for sequences in the Protein Databank (Bernstein *et al.*, 1977). *E*-values for 1ORD and 2DKB were 0.00006 and 0.0004, respectively; these values are the estimated probabilities of each sequence having been chosen by chance alone. The search also identified several other PLP-binding enzymes with significant scores, including tryptophanase (1AX4), aromatic amino acid aminotransferase (1AY4), tyrosine phenol-lyase (1TPL), and glutamate-1-semialdehyde aminomutase (2GSA), which were all shown to be close structural homologs to 2DKB using the Falicov & Cohen (1996) structural superposition algorithm. Earlier versions of the BLAST program (Altschul *et al.*, 1990) were unable to identify any significant matches.

Several functionally important residues are conserved across many decarboxylases and indicate the possibility of a highly conserved PLP-binding motif structure. These residues were used as anchors in the alignment to constrain the PLP-binding pocket and included: (1) active site residue K396 which forms a Schiff base with PLP. H395 and H282 which are possible proton donors in decarboxylases (Momany *et al.*, 1995a); (2) PLP interacting residues D364, W367, and S405, which may form hydrogen bonds to the -OH, -N1, and -OP group of PLP, respectively (Momany *et al.*, 1995a); (3) evolutionary-conserved regions G242GA, G337T, and W456 which may contribute to the structure of the PLP-binding pocket (Momany *et al.*, 1995b); and (4) substrate-interacting residue R558 which may form a hydrogen bond with a substrate (Toney *et al.*, 1995). Several of these residues (H282, D364, W367, G242, G337, R558) were aligned with their counterparts in the PSI-BLAST alignment. Deletions resulting in inter-C $^{\alpha}$ gaps of over 12 Å were not allowed in the automatic alignment, in order to facilitate model building. The region corresponding to residues 405-410 in GAD65 forms a beta strand in 1ORD, but was predicted to be a helix in GAD65. Because replacement of this strand with a helix would distort the PLP-binding site, the secondary structure prediction in this region was assumed to be incorrect. Therefore, the region between anchoring positions S405 and W456 was aligned to the 1ORD template using the original TOM program, (DeFay & Cohen 1996) so the incorrect secondary structure prediction in this region would not affect the alignment.

Automated model building from the templates was done using the program MODELLER (Sali & Blundell, 1993). Because insertions and deletions in loop regions were observed to distort parts of the core secondary structure, regions of sequence corresponding to known helices and strands in the template structures were con-

strained to remain helical or extended in the generated GAD65 structure. Several models were automatically generated; structurally reasonable backbones for the PLP and C-terminal domains which were consistent with the epitope data were chosen for further modeling. Side-chain positions were predicted with the SCWRL program (Bower *et al.*, 1997). The PLP-binding domain and C-terminal domains were manually docked using a connecting helix (residues 451-461) present in both template structures as a guide.

Acknowledgments

We thank Mr Jimmy Wu for help in generating mutants, Ms Katja Syren for help with antibody blocking studies and Dr Allan Tobin, University of California Los Angeles for the donation of cDNA for human GAD65 and GAD67. This work was supported by a Treadwell Foundation grant (S.B.), National Institutes of Health grants DK47043 and DK41822 (S.B.), a Human Frontier Science Program grant (S.B. and W.R.), a NIH-Immunology Training Grant (H.S.), and a Juvenile Diabetes Foundation International Fellowship Award (S.F.K.).

References

- Altschul, S. F., Gish, W., Miller, W., Myers, E. W. & Lipman, D. J. (1990). Basic local alignment search tool. *J. Mol. Biol.* **215**, 403-410.
- Altschul, S. F., Madden, T. L., Schaffer, A. A., Zhang, Z., Zhang, Z., Miller, W. & Lipman, D. J. (1997). Gapped BLAST and PSI-BLAST: a new generation of protein database search programs. *Nucl. Acids Res.* **25**, 3389-3402.
- Baekkeskov, S., Landin, M., Kristensen, J. K., Srikanta, S., Bruining, G. J., Mandrup, T., Poulson, T., Beaufort, C., Soeldner, J. S., Eisenbarth, G., Lindgren, F., Sundquist, G. & Lernmark, A. (1987). Antibodies to a Mr 64,000 human islet cell antigen precede the clinical onset of insulin-dependent diabetes. *J. Clin. Invest.* **79**, 926-934.
- Baekkeskov, S., Aanstoot, H. J., Christgau, S., Reetz, A., Solimena, M., Cascalho, M., Folli, F., Richter-Olesen, H. & De Camilli, P. (1990). The 64kD autoantigen in insulin-dependent diabetes is the GABA synthesizing enzyme glutamic acid decarboxylase. *Nature*, **347**, 151-156.
- Bernstein, F. C., Koetzle, T. F., Williams, G. J., Meyer, E. F., Brice, M. D., Rodgers, J. R., Kennard, O., Shimanouchi, T. & Tasumi, M. (1977). The Protein Data Bank: a computer based archival file for macromolecular structures. *J. Mol. Biol.* **112**, 535-542.
- Bower, M. J., Cohen, F. E., Dunbrack, J. & R., L. (1997). Prediction of protein sidechain conformations from a backbone-dependent rotamer library: a new homology modeling tool for proteins: application to side-chain prediction. *J. Mol. Biol.* **267**, 1268-1282.
- Bu, D. F. & Tobin, A. J. (1994). The exon-intron organization of the genes (GAD1 and GAD2) encoding two human glutamate decarboxylases (GAD67 and GAD65) suggests that they derive from a common ancestral GAD. *Genomics*, **21**, 222-228.
- Bu, D. F., Erlander, M. G., Hitz, B. C., Tillakaratne, N. J. K., Kaufman, D. L., Wagner-McPherson, C. B., Evans, G. A. & Tobin, A. J. (1992). Two human glutamate decarboxylases, 65-kDa Gad and 67-kDa

- GAD, are each encoded by a single gene. *Proc. Natl Acad. Sci. USA*, **89**, 2115-2119.
- Chandonia, J. M. & Karplus, M. (1999). New methods for accurate prediction of protein secondary structure. *Proteins: Struct. Funct. Genet.* **35**, 293-306.
- Chang, Y.-C. & Gottlieb, D. I. (1988). Characterization of the proteins purified with monoclonal antibodies to glutamic acid decarboxylase. *J. Neurosci.* **8**, 2123-2130.
- Christgau, S., Schierbeck, H., Aanstoot, H.-J., Aagaard, L., Begley, K., Kofod, H., Hejnaes, K. & Baekkeskov, S. (1991). Pancreatic β -cells express two autoantigenic forms of glutamic acid decarboxylase, a 65 kDa hydrophilic form and a 64 kDa amphiphilic form which can be both membrane-bound and soluble. *J. Biol. Chem.* **266**, 21257-21264.
- Christgau, S., Aanstoot, H.-J., Schierbeck, H., Begley, K., Tullin, S., Hejnaes, H. & Baekkeskov, S. (1992). Membrane anchoring of the autoantigen GAD65 to microvesicles in pancreatic β -cells by palmitoylation in the N-terminal domain. *J. Cell Biol.* **118**, 309-320.
- Christie, M. R., Daneman, D., Champagne, P. & Delovitch, T. L. (1990). Persistence of serum antibodies to 64,000-Mr islet cell protein after onset of type I diabetes. *Diabetes*, **39**, 653-656.
- Cunningham, B. C., Jhurani, P., Ng, P. & Wells, J. A. (1989). Receptor and antibody epitopes in human growth hormone identified by homolog-scanning mutagenesis. *Science*, **243**, 1330-1336.
- Defay, T. R. & Cohen, F. E. (1996). Multiple sequence information for threading algorithms. *J. Mol. Biol.* **262**, 314-323.
- Dunbrack, R. L. J., Gerloff, D. L., Bower, M., Chen, X., Lichtarge, O. & Cohen, F. E. (1997). Meeting Review: the Second meeting on the Critical Assessment of Techniques for Protein Structure Prediction (CASP2), Asilomar, California, December 13-16, 1996. *Fold. Design*, **2**, R27-42.
- Endl, J., Otto, H., G., J., Dreisbusch, B., Donie, F., Stahl, P., Elbracht, R., Schmitz, G., Mein, E., Hummel, M., Ziegler, A.-G., Wank, R. & Schendel, D. J. (1997). Identification of naturally processed T-cell epitopes from glutamic acid decarboxylase presented in the context of HLA-DR alleles by T lymphocytes of recent onset IDDM patients. *J. Clin. Invest.* **10**, 1-11.
- Erlander, M. G., Tillakaratne, N. J. K., Feldblum, S., Patel, N. & Tobin, A. J. (1991). Two genes encode distinct glutamate decarboxylases. *Neuron*, **7**, 91-100.
- Falicov, A. & Cohen, F. E. (1996). A surface of minimum area metric for the structural comparison of proteins. *J. Mol. Biol.* **258**, 871-892.
- Hagopian, W. A., Michelsen, B., Karlsen, A. E., Larsen, F., Moody, A., Grubin, C. E., Rowe, R., Petersen, J., McEvoy, R. & Lernmark, A. (1993). Autoantibodies in IDDM primarily recognize the 65,000-M(r) rather than the 67,000-M(r) isoform of glutamic acid decarboxylase. *Diabetes*, **42**, 631-636.
- Hensch, T. K., Fagiolini, M., Mataga, N., Stryker, M. P., Baekkeskov, S. & Kash, S. (1998). Rapid GABA-release is involved in development of plasticity in the visual cortex. *Science*, **282**, 1504-1508.
- Kash, S. F., Johnson, R. S., Tecott, L. H., Noebels, J. L., Mayfield, R. D., Hanahan, D. & Baekkeskov, S. (1997). Epilepsy in mice deficient in the 65-kDa isoform of glutamic acid decarboxylase. *Proc. Natl Acad. Sci. USA*, **94**, 14060-14065.
- Kash, S. F., Tecott, L. H., Hodge, C. & Baekkeskov, S. (1999). Increased anxiety and altered responses to anxiolytics in mice deficient in the 65-kDa isoform of glutamic acid decarboxylase. *Proc. Natl Acad. Sci. USA*, **96**, 1698-1703.
- Kaufman, D. L., Houser, C. R. & Tobin, A. J. (1991). Two forms of the γ -Aminobutyric acid synthetic enzyme glutamate decarboxylase have distinct intraneuronal distributions and cofactor interactions. *J. Neurochem.* **56**, 720-723.
- Kaufman, D. L., Clare-Salzler, M., Tian, J., Forsthuber, T., Ting, G. S. P., Robinson, P., Atkinson, M. A., Sercarz, E. E., Tobin, A. J. & Lehmann, P. V. (1993). Spontaneous loss of T-cell tolerance to glutamic acid decarboxylase in murine insulin-dependent diabetes. *Nature*, **366**, 69-72.
- Kim, J., Namchuk, M., Bugawan, D., Fu, Q., Jaffe, M., Shi, Y., Aanstoot, H.-J., Turck, C., Erlich, H., Lennon, V. & Baekkeskov, S. (1994). Higher autoantibody levels and recognition of a linear N-terminal epitope in the autoantigen GAD65 distinguish stiff-man syndrome from insulin dependent diabetes mellitus. *J. Exp. Med.* **180**, 595-606.
- Kunkel, T. A., Roberts, J. D. & Zakour, R. A. (1987). Rapid and efficient site-specific mutagenesis without phenotypic selection. *Methods Enzymol.* **154**, 367-382.
- Laemmli, U. K. (1970). Cleavage of structural proteins during the assembly of the head of bacteriophage T4. *Nature*, **227**, 680-685.
- Lorish, T. R., Thorsteinssen, G. & Howard, F. M. (1989). Stiff-man syndrome updated. *Mayo Clin. Proc.* **64**, 629-636.
- Maced, A.-M., Rousset, F., Ho, S., Robert, F., Thivolet, C., Orgiazzi, J. & Lebecque, S. (1996). Four IgG anti-islet human monoclonal antibodies isolated from a type 1 diabetes patient recognize distinct epitopes of glutamic acid decarboxylase 65 and are somatically mutated. *J. Immunol.* **156**, 3541-3549.
- Martin, J. M. & Lacey, P. E. (1963). The prediabetic period in partially pancreatectomized rats. *Diabetes*, **12**, 238-242.
- Miyazawa, S. & Jernigan, R. L. (1985). Estimation of effective interresidue contact energies from protein crystal structures: quasi-chemical approximation. *Macromolecules*, **18**, 534-552.
- Momany, C., Ernst, S., Ghosh, R. & Hackert, M. L. (1995a). Crystallographic structure of a PLP-dependent ornithine decarboxylase from *Lactobacillus* 30a to 3.0 Å resolution. *J. Mol. Biol.* **252**, 643-655.
- Momany, C., Ghosh, R. & Hackert, M. L. (1995b). Structural motifs for pyridoxal-5'-phosphate binding in decarboxylases: an analysis based on the crystal structure of the *Lactobacillus* 30a ornithine decarboxylase. *Protein Sci.* **4**, 849-854.
- Patel, S. D., Cope, A. P., Congia, M., Chen, T. T., Kim, E., Fugger, L., Wherret, D. & Sonderstrup-McDevitt, G. (1997). Identification of immunodominant T-cell epitopes of human glutamic acid decarboxylase 65 by using HLA-DR (α 1*0101, β 1*0401) transgenic mice. *Proc. Natl Acad. Sci. USA*, **15**, 8082-8087.
- Perrin, S. & Gilliland, G. (1990). Site-specific mutagenesis using asymmetric polymerase chain reaction and a single mutant primer. *Nucl. Acids Res.* **18**, 7433-7438.
- Petersen, J. S., Hejnaes, K. R., Moody, A., Karlsen, A. E., Marshall, M. O., Hoier-Madsen, M., Boel, E., Michelsen, B. K. & Dyrberg, T. (1994). Detection of GAD65 antibodies in diabetes and other autoimmune diseases using a simple radioligand assay. *Diabetes*, **43**, 459-467.

- Reetz, A., Solimena, M., Matteoli, M., Folli, F., Takei, K. & DeCamilli, P. (1991). GABA and pancreatic β -cells: colocalization of glutamic acid decarboxylase (GAD) and GABA with synaptic like microvesicles suggests their role in GABA storage and secretion. *EMBO J.* **10**, 1275-1284.
- Richter, W., Shi, Y. & Baekkeskov, S. (1993). Autoreactive epitopes in glutamic acid decarboxylase defined by diabetes-associated human monoclonal antibodies. *Proc. Natl Acad. Sci. USA*, **90**, 2832-2836.
- Ridsdale, R. A., Beniac, D. R., Tompkins, T. A., Moscarello, M. A. & Harauz, G. (1997). Three-dimensional structure of myelin basic protein. *J. Biol. Chem.* **272**, 4269-4275.
- Sali, A. & Blundell, T. L. (1993). Comparative protein modelling by satisfaction of spatial restraints. *J. Mol. Biol.* **234**, 779-815.
- Sandmeier, E., Hale, T. I. & Christen, P. (1994). Multiple evolutionary origin of pyridoxal-5'-phosphate-dependent amino acid decarboxylases. *Eur. J. Biochem.* **221**, 997-1002.
- Schagger, H. & von Jagow, G. (1987). Tricine-sodium dodecyl sulfate-polyacrylamide gel electrophoresis for the separation of proteins in the range from 1 to 100 kDa. *Anal. Biochem.* **166**, 368-379.
- Sheikh, S. N. & Martin, D. L. (1996). Elevation of brain GABA levels with vigabatrin (γ -vinyl GABA) differentially affects GAD65 and GAD67 expression in various regions of rat brain. *J. Neurosci. Res.* **52**, 736-741.
- Shi, Y., Veit, B. & Baekkeskov, S. (1994). Amino acid residues 24-31 but not palmitoylation of cysteines 30 and 45 are required for membrane anchoring of glutamic acid decarboxylase, GAD65. *J. Cell Biol.* **124**, 927-934.
- Simitsek, P. D., Campbell, D. G., Lanzavecchia, A., Fairweather, N. & Watts, C. (1995). Modulation of antigen processing by bound antibodies can boost or suppress class II major histocompatibility complex presentation of different T-cell determinants. *J. Exp. Med.* **181**, 1957-1963.
- Solimena, M., Folli, F., Aparisi, R., Pozza, G. & De Camilli, P. (1990). Autoantibodies to GABA-ergic neurons and pancreatic β -cells in stiff-man syndrome. *N. Engl. J. Med.* **322**, 1555-1560.
- Syren, K., Lindsay, L., Stoehrer, B., Jury, K., Luhder, F., Baekkeskov, S. & Richter, W. (1996). Immune reactivity of diabetes associated human monoclonal antibodies defines multiple epitopes and detects two domain boundaries in glutamate decarboxylase. *J. Immunol.* **157**, 5208-5214.
- Taylor, W. R. (1989). A template based method of pattern matching in protein sequences. *Prog. Biophys. Mol. Biol.* **54**, 159-252.
- Thompson, J. D., Higgins, D. G. & Gibson, T. J. (1994). CLUSTAL W: improving the sensitivity of progressive multiple sequence alignment through sequence weighting, positions-specific gap penalties and weight matrix choice. *Nucl. Acids Res.* **22**, 4673-4680.
- Tian, J., Lehmann, P. V. & Kaufman, D. L. (1994). T-cell cross-reactivity between coxsackievirus and glutamate decarboxylase is associated with a murine diabetes susceptibility allele. *J. Exp. Med.* **180**, 1979-1984.
- Tisch, R., Yang, X.-D., Singer, S. M., Liblau, R. S., Fugger, L. & McDevitt, H. O. (1993). Immune response to glutamic acid decarboxylase correlates with insulinitis in non-obese diabetic mice. *Nature*, **366**, 72-75.
- Toney, M. D., Hohenester, E., Keller, J. W. & Jansonius, J. N. (1995). Structural and mechanistic analysis of two refined crystal structures of the pyridoxal phosphate-dependent enzyme dialkylglycine decarboxylase. *J. Mol. Biol.* **245**, 151-179.
- Tremble, J., Morgenthaler, N. G., Vlug, A., Powers, A. C., Christie, M. R., Scherbaum, W. A. & Banga, J. P. (1997). Human B cells secreting immunoglobulin G to glutamic acid decarboxylase-65 from a nondiabetic patient with multiple autoantibodies and Graves' Disease: a comparison with those present in type 1 diabetes. *J. Clin. Endocrinol. Metab.* **82**, 2664-2670.
- Wicker, L. S., Chen, S. L., Nepom, G. T., Elliott, J. F., Freed, D. C., Bansal, A., Zheng, S., Herman, A., Lernmark, A., Zaller, D. M., Peterson, L. B., Rothbard, J. B., Cummings, R. & Whiteley, P. J. (1996). Naturally processed T-cell epitopes from human glutamic acid decarboxylase identified using mice transgenic for the type 1 diabetes-associated human MHC class II allele, DRB1*0401. *J. Clin. Invest.* **98**, 2597-2603.
- Wucherpfennig, K. W., Catz, I., Hausmann, S., Strominger, J. L., Steinman, L. & Warren, K. G. (1997). Recognition of the immunodominant myelin basic protein peptide by autoantibodies and HLA-DR2-restricted T-cell clones from multiple sclerosis patients. Identity of key contact residues in the B-cell and T-cell epitopes. *J. Clin. Invest.* **100**, 1114-1122.
- Zekzer, D., Wong, F. S., Ayalon, O., Millet, I., Altieri, M., Shintani, S., Solimena, M. & Sherwin, R. S. (1998). GAD-reactive CD4+ Th1 cells induce diabetes in NOD/SCID mice. *J. Clin. Invest.* **101**, 68-73.

Edited by J. A. Wells

(Received 9 November 1998; received in revised form 20 February 1999; accepted 24 February 1999)